Magnetic-field asymmetry of nonlinear mesoscopic transport

David Sánchez and Markus Büttiker

Département de Physique Théorique, Université de Genève, CH-1211 Genève 4, Switzerland

(Dated: February 2, 2008)

We investigate departures of the Onsager relations in the nonlinear regime of electronic transport through mesoscopic systems. We show that the nonlinear current-voltage characteristic is not an even function of the magnetic field due only to the magnetic-field dependence of the screening potential within the conductor. We illustrate this result for two types of conductors: A quantum Hall bar with an antidot and a chaotic cavity connected to quantum point contacts. For the chaotic cavity we obtain through random matrix theory an asymmetry in the fluctuations of the nonlinear conductance that vanishes rapidly with the size of the contacts.

Introduction.—The Onsager-Casimir relations [1, 2] are symmetry conditions for correlation functions. These can be cast as friction coefficients by means of the fluctuation-dissipation theorem. In electronic transport measurements, the information about dissipation is carried by the conductance of the sample. Microscopic reversibility thus requires that in the presence of a magnetic field B the conductance obeys $G_{\alpha\beta}(B) = G_{\beta\alpha}(-B)$ between contacts α and β. In particular, for a two-probe conductor the conductance is an even function of magnetic field $G(B) = G(-B)$. Such relations generally hold for *macroscopic* systems near thermodynamic *equilibrium.* What happens when these conditions are not fulfilled? First, when transport is phase coherent as it occurs in *mesoscopic* conductors, the conductance is not just material specific but also depends on the probe configuration. Then, a generalized reciprocity theorem may be proved provided current and voltage probes are treated on equal footing [3]. Second, away from equilibrium (e.g., in *nonlinear* dc-transport) there are no fundamental reasons why the Onsager relations should hold. In particular, in a two terminal conductor, we can expect that the nonlinear I–V characteristic is not an even function of magnetic field, $I(B, V) \neq I(-B, V)$. Below, we demonstrate that such asymmetries can indeed be found but importantly only to the extent that the potential landscape in the interior of the conductor becomes an uneven function of magnetic field [4].

Nonlinear transport in mesoscopic conductors is a subject of growing interest. Rectification effects in asymmetric microjunctions [5], quantum point contacts [6], and switching and gain in three-terminal ballistic branches [7] have been observed. For samples with special spatial symmetries, a set of symmetry relations which hold in the nonlinear regime have been discussed and experimentally verified by Löfgren *et al.* [8] Conductance fluctuations away from equilibrium have long been of theoretical [9] and experimental [10, 11] concern. Recently, Zumbühl, Marcus *et al.* [12] started experiments to investigate the magnetic-field symmetry of fluctuations away from equilibrium.

A correct treatment of this problem requires a *self-consistent* discussion of the screening potential within the conductor. A scattering picture of weakly nonlinear transport was provided by Christen and Büttiker [4, 13]. The work of Sheng *et al.* [14] exemplifies a computational implementation. We briefly now discuss the essential elements of this approach.

Consider a mesoscopic conductor penetrated by a magnetic field B perpendicular to the plane of the sample and connected to $\alpha = 1, \ldots, M$ reservoirs and gates. Transport is described by the scattering matrix $s_{\alpha\beta}$. For purely elastic transport, the scattering matrix is a function of the energy E of the carriers and it is a functional of the potential landscape $U(\vec{r})$ of the conductor, $s_{\alpha\beta}[E; U(\vec{r})]$. For linear transport, the scattering matrix is evaluated at the equilibrium potential $U_{\text{eq}}(\vec{r})$ which is an even function of B. As a consequence, $s_{\alpha\beta}(B) = s_{\beta\alpha}(-B)$ at equilibrium. Away from equilibrium the potential depends on the voltages V_α (measured from an equilibrium chemical potential μ_0) applied to the leads and the nearby gates. We can write $U(\vec{r}) = U_{\text{eq}}(\vec{r}) + \sum_\alpha u_\alpha V_\alpha + \mathcal{O}(V^2)$. Here, the characteristic potentials (CP's) $u_\gamma(\vec{r}) = [\partial U(\vec{r})/\partial V_\gamma]_{\text{eq}}$ relate the variation of $U(\vec{r})$ in the sample to a voltage shift in the contact γ [4]. We expand the current through lead α in powers of the voltage shifts up to second order:

$$I_\alpha = \sum_\beta G_{\alpha\beta} V_\beta + \sum_{\beta\gamma} G_{\alpha\beta\gamma} V_\beta V_\gamma. \qquad (1)$$

The linear conductances are expressed by the well known formula $G_{\alpha\beta} = (e^2/h) \int dE[-\partial_E f(E - \mu_0 - V_\alpha)] A_{\alpha\beta}(E; \{V_\alpha\} = 0)$, where $f(E)$ is the Fermi function and $A_{\alpha\beta}(E; \{V_\alpha\}) = \text{Tr}[1_{\alpha\beta}\delta_{\alpha\beta} - s_{\alpha\beta}^\dagger s_{\alpha\beta}]$. The second-order nonlinearity $G_{\alpha\beta\gamma}$ contains information about the charge *response* of the system. Reference [13] finds:

$$G_{\alpha\beta\gamma} = \frac{e^2}{h} \int dE \, \frac{\partial f}{\partial E} \int d^3r \, \frac{\delta A_{\alpha\beta}}{\delta U(\vec{r})}[\delta_{\beta\gamma} - 2u_\gamma(\vec{r})]. \quad (2)$$

Here the nonequilibrium state is described by the CP's, u_β, which arise as a consequence of screening of the additional bare charge injected from contact β. This charge

density of states (DOS) is the injectivity [4] of contact β,

$$\frac{d\bar{n}_\beta(\vec{r})}{dE} = -\frac{1}{2\pi i}\sum_\alpha \text{Tr}\left(s_{\alpha\beta}^\dagger \frac{\delta s_{\alpha\beta}}{e\delta U(\vec{r})}\right). \qquad (3)$$

On the other hand, the additional current in contact β due to a variation of the screening potential at point $\vec{r}$, is given by the emissivity into β, $d\underline{n}_\beta(\vec{r})/dE$. Due to microreversibility, $d\bar{n}_\beta(B,\vec{r})/dE = d\underline{n}_\beta(-B,\vec{r})/dE$. However, neither the injectivity nor the emissivity alone are invariant under B-reversal. As a result, the CP's are *not* even functions of B. Thus, quite generally, even in a two-terminal setup the second-order contribution $G_{\alpha\beta\gamma}$ to the I–V characteristic is not even in the field. We define the magnetic-field asymmetry for such a setup:

$$\Phi = \frac{1}{2}[G_{111}(B) - G_{111}(-B)]. \qquad (4)$$

We emphasize that the asymmetry $\Phi \neq 0$ is generated in Eq. (2) only through the asymmetry in the electric potential: if the potential is even in B, Eq. (2) predicts for a two-terminal conductor a current that is even. Thus, a self-consistent description of charge redistribution is crucial.

Our purpose is to elucidate this general result with the help of a simple but instructive example (a quantum Hall bar with an antidot) and to provide a prediction of the size of Φ for a generic conductor, a chaotic cavity.

Quantum Hall bar.—We consider a conductor in the quantum Hall regime as depicted in the left panel of Fig. 1. Edge states are symbolically indicated by arrows along the upper and lower edge of the sample. For simplicity, we assume that B is so strong that only the lowest Landau level is occupied (filling factor $\nu = 1$). Backscattering is achieved by producing with gates a potential hill, thus forming an antidot [15]. The antidot behaves effectively like a quantum impurity with a Breit-Wigner resonance at $E_0 + eU_d$ coupled to the edge states via
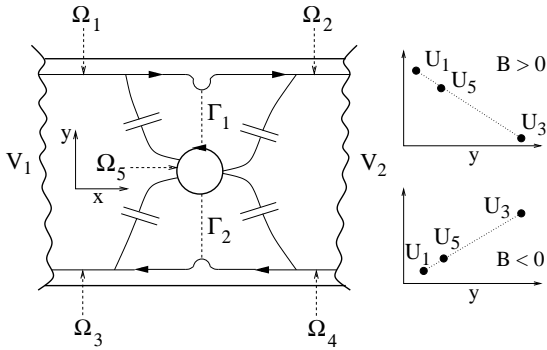

FIG. 1: Left panel: quantum Hall conductor attached to two reservoirs with an antidot connecting two edge states. Right panel: Schematic spatial variation of the screening potential inside the bar for opposite polarities of the magnetic field.

hybridization widths Γ_1 and Γ_2 due to tunneling. Both broadenings are taken to be energy independent. U_d is the potential at the antidot.

Let us first provide an intuitive picture of the nonlinear transport. Application of a voltage $V_1 > V_2$, leads to an excess charge on the upper edge, and through screening to a corresponding deficit of charge on the lower edge. Hence, a Hall potential $U_H(B,\vec{r})$ is established. The charges on the edge state lifts the resonant energy to a value $E_0 + eU_d(B)$ (upper right panel of Fig. 1). If we now reverse the field, it is the lower edge state that is charged, and the upper edge state that is lowered in energy through screening, generating an electric field opposite to that of $U_H(B)$. Then, the resonant energy will now be at $E_0 + eU_d(-B)$ (lower right panel of Fig. 1). Clearly, $eU_d(B)$ and $eU_d(-B)$ will in general not be equal, except if stringent symmetry conditions are fulfilled. The symmetry is broken either through *scattering asymmetry*, i.e., if transmission into the antidot is not symmetric $\Gamma_1 \neq \Gamma_2$, or through *electrical asymmetry* if the charges on the upper edge couple more strongly to the antidot than the charges on the lower edge.

We now support this picture with analytical calculations. Evaluation of the exact local potential distribution can typically be achieved only computationally. To simplify the problem, we divide the conductor into five regions Ω_i with $i = 1,\ldots,5$ as indicated in Fig. 1. $\Omega_5 \equiv \Omega_d$ is the region of the edge state circling the antidot. In each region the potential is taken to be constant. Interaction between charges in different regions is described by a geometric capacitance matrix C_{ij}. Such a *discrete* potential model captures the essential physics [4, 13]. Thus, the CP in region i is $u_{i\gamma} = \partial U_i/\partial V_\gamma$ and the injectivity of lead α into region i is $\bar{D}_{i\alpha} = \int_{\Omega_i} d^3r\, d\bar{n}_\alpha(\vec{r})/dE$. When the energy is close to $E_0 + eU_d$ an electron is reflected through the antidot (e.g., from Ω_1 to Ω_3) with a probability $R = 1 - T = \Gamma_1\Gamma_2/|\Delta|^2$, where $\Delta = \mu_0 - E_0 - eU_5 + i\Gamma/2$ with $\Gamma = \Gamma_1 + \Gamma_2$ as the total linewidth. Using the corresponding scattering matrix we find the injectivities into the different regions. For the case $B > 0$ (Fig. 1, left panel) the DOS associated to carriers at Ω_3 injected by lead 1 reads $\bar{D}_{31} = D_3 R$, where D_i is the total (B-dependent) DOS of the upper edge state in region i. Similarly, the remaining injectivities of contact 1 are $\bar{D}_{11} = D_1$, $\bar{D}_{21} = D_2 T$, $\bar{D}_{41} = 0$ and $\bar{D}_{51} = e^2\Gamma_1/2\pi|\Delta|^2$. One proceeds likewise to find the injectivities of contact 2, $\bar{D}_{i2}$. The charge q_i in region i can be expressed in two ways:

$$q_i = e^2\sum_\alpha \bar{D}_{i\alpha}(V_\alpha - U_i) = \sum_j C_{ij}U_j. \qquad (5)$$

First, q_i is the bare injected charge due to the voltage applied to the contact and the screening charge induced by the internal potential U_i. Second, q_i is the charge permitted by the Coulomb interaction, where C_{ij} is the geometrical capacitance matrix whose indices run over all (five) regions considered in Fig. 1. Equation (5) al-

lows us to determine the potentials U_i as a function of the applied voltages. We take equal DOS for all regions $D_i = D$. We consider separately the case of (A) an electrically symmetric sample that is asymmetric only in the scattering properties and (B) the case of a sample with symmetric scattering that is asymmetric only electrically.

For case (A) we assume a capacitance matrix with equal capacitances C between the edge states and the antidot. Transmission from the antidot to the upper and lower edge state is asymmetric $\eta = (\Gamma_1 - \Gamma_2)/\Gamma$. Using Eq. (2) and Eq. (5) we evaluate the second-order nonlinear conductance and insert it in Eq. (4). Taking into account that the transmission (reflection) probabilities depend only on the potential at the antidot, and that $\delta T/e\delta U_d = -dT/dE|_{E_F}$ at zero temperature, we find

$$\Phi = -\frac{e^3}{h}\left.\frac{dT}{dE}\right|_{\rm eq}\frac{\eta R(C + e^2 D)}{2\pi CD\Gamma + R(C + e^2 D)} + \mathcal{O}(\eta^3). \quad (6)$$

We observe that in the charge neutral limit ($C = 0$) the magnetic-field asymmetry Φ is independent of R (to leading order in η). In the noninteracting limit ($C \to \infty$), the asymmetry is proportional to $R/(R + 2\pi D\Gamma)$.

Next consider case (B), a sample with symmetric scattering properties ($\eta = 0$) but being electrically asymmetric. Such a case arises if the tunnel barrier separating the antidot from the top edge state is not very high in energy but wide whereas the barrier separating the antidot from the lower edge state is high in energy but narrow such that transmission through both is equal. However, the capacitance to the upper $(1+\xi)C$ and lower $(1-\xi)C$ edge states will differ, ξ being a dimensionless parameter. As above, we calculate the B-dependent second-order conductance to lowest order in ξ to find:

$$\Phi = -\frac{e^3}{h}\left.\frac{dT}{dE}\right|_{\rm eq}\frac{\pi\xi e^2 D^2 C\Gamma T}{(C + e^2 D)[2\pi CD\Gamma + R(C + e^2 D)]}. \quad (7)$$

Interestingly, the magnetic-field asymmetry is proportional to the transmission probability T, unlike case (A). Thus, the transmission of the impurity would act experimentally as the indicator of the physical mechanism behind the resulting field asymmetry.

Our discussion demonstrates that either asymmetric scattering or an electrical asymmetry generates already to second order in voltage a deviation from the Onsager relations that hold in the linear regime. For strong backscattering, this deviation is due mainly to a scattering induced asymmetry whereas for weakly coupled impurities the electric asymmetry dominates.

Chaotic cavity.—It is important to find out whether such symmetry breaking is only relevant for few-channel problems or whether in fact symmetry breaking is also observable in the many-channel limit. This is the motivation to investigate now a chaotic cavity, which is a metallic quantum dot whose classical analog displays chaotic

dynamics. For clean samples the transport within the cavity is ballistic and its corresponding statistics is well described by random matrix theory [16]. Open cavities have been extensively studied both theoretically [17] and experimentally [18]. Most of these works are restricted to the linear conductance regime (see, however, Ref. [8]). The chaotic cavity is coupled to reservoirs ($\alpha = 1, 2$) through quantum point contacts with N_1 and N_2 propagating channels (left inset of Fig. 2). On the ensemble average such a cavity exhibits simply a linear I–V characteristic with a conductance $G = e^2 N_1 N_2/hN$ where $N = N_1 + N_2$. Nonlinearities arise due to quantum fluctuations with an energy scale equal to the Thouless energy $E_T = N\delta$ with δ the mean level spacing.

Since a cavity is effectively zero-dimensional due to its isotropic properties, we take into account screening with a single potential U. Surrounding gates are coupled capacitively with a gate voltage V_g and a geometric capacitance C. In response to a shift of the contact voltages V_α a nonequilibrium charge builds up in the cavity which depends on the injecting contact. The two equations which determine the excess charge on the cavity are

$$Q = \sum_\alpha e^2 \bar{D}_\alpha(V_\alpha - U) = C(U - V_g), \quad (8)$$

where, as before, $\bar{D}_\alpha$ is the injectivity of lead α. The total DOS of the cavity is $D = \sum_\alpha \bar{D}_\alpha$.

As we have now a three-terminal problem with a gate voltage $V_3 = V_g$, we consider the case where $V_3 = V_2$. From Eq. (2) we get $I_1 = G_{11}(V_1 - V_2) + G_{111}(V_1 - V_2)^2 + \mathcal{O}(V^3)$. Using the WKB approximation, we can again replace derivatives with regard to potentials by energy derivatives [13] and find

$$G_{111} = -\frac{e^3}{h}\left.\frac{dT}{dE}\right|_{\rm eq}(1 - 2u_1). \quad (9)$$
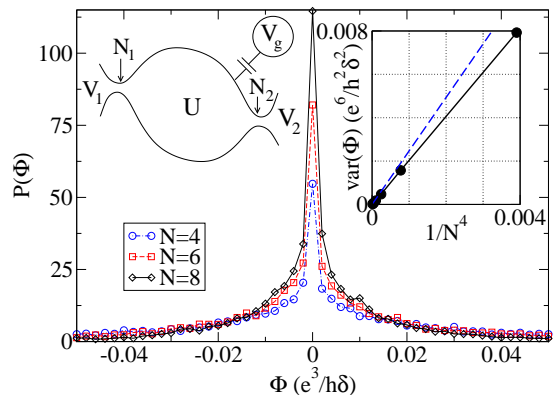

FIG. 2: (Color online). Normalized probability densities for the magnetic-field asymmetry Φ of a chaotic cavity connected to two reservoirs (left inset). Right inset: fluctuations of Φ as a function of the total number of modes N. The dashed line is the analytical prediction for $N \gg 1$.

For the chaotic cavity the ensemble average $\langle G_{111} \rangle = 0$ vanishes, an asymmetry can develop only due to quantum *fluctuations*. We now show that var(Φ) is nonzero.

For $N_1 \gg 1$ and $N_2 \gg 1$ within random matrix theory the product in the right hand side of Eq. (9) can be decoupled [17]. Thus, we disregard correlations between dT/dE and u_1. The *unscreened* nonlinear conductance $-(e^3/h)dT/dE|_{\rm eq}$ changes sign randomly on the ensemble so that its average is zero [19]. In the unitary ensemble (magnetic flux through the cavity of the order of 1 quantum) we find for the fluctuations $\mathrm{var}(dT/dE) = 8\pi^2 N_1^2 N_2^2 / N^6 \delta^2$. Furthermore, we neglect the small fluctuations [20] in the electrochemical capacitance $1/C_\mu = 1/C + \delta/e^2$. Then, from Eq. (8) and Eq. (9) we find that the fluctuations of u_1 are determined by the fluctuations of the asymmetric part of the injectivity. Correlations of injectivities have been investigated in Ref. [20]. Using these results in Eq. (4) we find

$$\mathrm{var}(\Phi) = \frac{e^6}{h^2 \delta^2} \frac{16\pi^2 N_1^3 N_2^3}{N^{10}} \left(\frac{C_\mu}{C} \right)^2 . \qquad (10)$$

The fluctuations go as $1/N^4$ for $N \gg 1$, thus vanishing quickly with increasing number of channels and are maximal for perfect screening $C_\mu = C$.

For small N_1 and N_2 a full analytical calculation of var(Φ) is involved since one has to evaluate high-order correlations between D_α, D, and dT/dE. Yet, we can substantiate Eq. (10) with numerical calculations. The results for $C = 0$ and $N_1 = N_2 = N/2$ are shown in Fig. 2. In these simulations, the S matrix is expressed in terms of the Hamiltonian matrix of the cavity, whose elements are random from the unitary ensemble [17]. From the resulting S and dS/dE we compute the distribution of Φ. We observe that the probability density of Φ is a narrow peak centered around zero. The variance decreases quickly with N (see the right inset). Strikingly, the fluctuations are in good agreement (within the numerical error) with the analytical prediction (10). These results demonstrate unambiguously that the fluctuations of the nonlinear conductance of a chaotic cavity are not symmetric under field reversal and that they depend strongly on the fluctuations of the screening potential.

In single-channel conductors, the asymmetry is large [var(Φ) $\simeq 0.2(e^3/h\delta)^2$ for $N = 2$, not shown in Fig. 2] and of the same order as a linear conductance fluctuation. But as the number of channels increases the asymmetry rapidly becomes much smaller than a linear conductance fluctuation or weak localization correction due to the smallness of the DOS fluctuations [20]. Therefore, experiments on few-channel conductors are most promising for the detection of the asymmetry described here.

Conclusion.—We have investigated departures from the Onsager relations in mesoscopic systems in the nonlinear regime. Because of the screening potential, the weakly nonlinear conductance is asymmetric under magnetic-field reversal. We have determined the conditions under which such departures are experimentally observed. Our approach can be applied to systems that exhibit similar phenomena such as metallic nanowires [21] and molecular junctions [22].

Note added.—During completion of this work we became aware of related work by B. Spivak and A. Zyuzin [23] treating a diffusive cavity.

[1] L. Onsager, Phys. Rev. **38**, 2265 (1931).
[2] H.B.G. Casimir, Rev. Mod. Phys. **17**, 343 (1945).
[3] M. Büttiker, Phys. Rev. Lett. **57**, 1761 (1986).
[4] M. Büttiker, J. Phys.: Condens. Matter **5**, 9361 (1993).
[5] A. M. Song *et al.*, Phys. Rev. Lett. **80**, 3831 (1998).
[6] I. Shorubalko *et al.*, Appl. Phys. Lett. **79**, 1384 (2001).
[7] S. Reitzenstein *et al.*, Phys. Rev. Lett. **89**, 226804 (2002).
[8] A. Löfgren *et al.*, Phys. Rev. Lett. **92**, 046803 (2004).
[9] B.L. Al'tshuler and D.E. Khmel'nitskii, JETP Lett. **42**, 359 (1986).
[10] R.A. Webb, S. Washburn, and C. P. Umbach, Phys. Rev. B **37**, 8455 (1988).
[11] R. Taboryski *et al.*, Phys. Rev. B **49**, 7813 (1994).
[12] D.M. Zumbühl, C.M. Marcus, M. Hanson, and A.C. Gossard (unpublished).
[13] T. Christen and M. Büttiker, Europhys. Lett. **35**, 523 (1996).
[14] W. Sheng *et al.*, Phys. Rev. B **59**, 538 (1999).
[15] C.J.B. Ford *et al.*, Phys. Rev. B **49**, 17456 (1994); G. Kirczenow, *et al.*, Phys. Rev. Lett. **72**, 2069 (1994).
[16] H.U. Baranger and P.A. Mello, Phys. Rev. Lett. **73**, 142 (1994); R.A. Jalabert, J.-L. Pichard, and C.W.J. Beenakker, Europhys. Lett. **27**, 255 (1994).
[17] C.W.J. Beenakker, Rev. Mod. Phys. **69**, 731 (1997).
[18] A.G. Huibers *et al.*, Phys. Rev. Lett. **81**, 1917 (1998).
[19] M.L. Polianski and P.W. Brouwer, J. Phys. A: Math. Gen. **36**, 3215 (2003).
[20] P.W. Brouwer and M. Büttiker, Europhys. Lett. **37**, 441 (1997).
[21] N. Agrait, A.L. Yeyati, and J.M. van Ruitenbeek, Phys. Rep. **377**, 81 (2003).
[22] P. Pomorski *et al.*, Phys. Rev. B **69**, 115418 (2004).
[23] B. Spivak and A. Zyuzin, cond-mat/0404408.